

The Effect of Realism on Hand Redirection in Immersive Environments

Shuqi Liao , Yuqi Zhou , and Voicu Popescu 

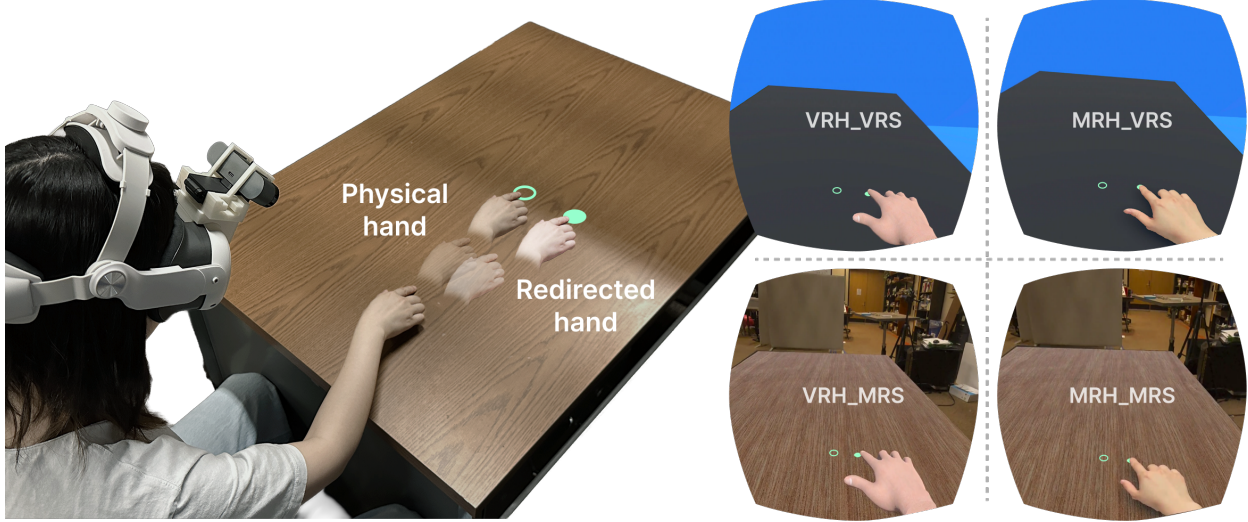


Fig. 1: Hand redirection in four conditions. *Left*: a participant wearing an XR headset reaches out to touch a virtual target (green dot); redirection is applied so that when the participant sees their hand touch the virtual target, their physical hand touches an offset physical target (green circle, not visible to the participant, shown here for illustration purposes). *Right*: first person views of the four conditions of our user study, combining two hand rendering modes—one using a generic VR avatar hand (VRH) and one a photorealistic model based on a live video frame (MRH)—and two scene rendering modes—one using a virtual environment (VRS) and one the actual physical surroundings of the user in video passthrough mode (MRS).

Abstract—Redirection in virtual reality (VR) enhances haptic feedback versatility by relaxing the need for precise alignment between virtual and physical objects. In mixed reality (MR), where users see the real world and their own hands, haptic redirection enables a physical interaction with virtual objects but poses greater challenges due to altering real-world perception. This paper investigates the effect of the realism of the user’s surroundings and of the user’s hand on haptic redirection. The user’s familiarity with their actual physical surroundings and their actual hand could make the redirection manipulations easier—or harder—to detect. In a user study ($N = 30$) participants saw either a virtual environment or their actual physical surroundings, and saw their hand rendered either with a generic 3D model or with a live 2D video sprite of their actual hand. The study used a two-alternative forced choice (2AFC) design asking participants to detect hand redirections that bridged physical to virtual offsets of varying magnitudes. The results show that participants were not more sensitive to 2D video sprite hand redirection than to VR hand redirection, which supports the use of haptic redirection in MR.

Index Terms—Hand redirection, mixed reality, haptic feedback, hand tracking

1 INTRODUCTION

Haptic feedback greatly enhances virtual reality (VR) applications by allowing users not just to see but also to feel the virtual objects with which they interact [53, 56, 63]. Providing convincing haptic feedback is challenging. One approach is to rely on physical objects in the user’s surroundings to impersonate the virtual objects with which the user interacts [28, 41]. The approach provides limited haptic feedback opportunities since it is unlikely that the user’s physical surroundings match the virtual world. The number of haptic feedback opportunities

has been increased by using redirection to tolerate offsets between physical and virtual objects, such that the same physical object can be used to provide haptic feedback for multiple virtual objects [1, 25, 35, 66]. Redirection has to accommodate two competing requirements: the offset between real and virtual should be large in order to provide haptic feedback in a wide range of scenarios, and, at the same time, the offset should be small enough for it to go unnoticed by the user [64, 68, 69].

Advances in video passthrough headset technology (e.g., Oculus Quest 3¹, HTC Vive², and Apple Vision Pro³) support mixed reality (MR) immersive visualization applications where users see their actual hands and their actual physical surroundings into which virtual objects are integrated seamlessly [33]. Like in VR, haptic redirection is called upon to allow users to touch the virtual objects of an MR application. Unlike in VR, haptic redirection is more challenging in MR as one has to manipulate the user’s view of their physical surroundings.

• Shuqi Liao is with Purdue University. E-mail: liao201@purdue.edu.

• Yuqi Zhou is with Purdue University. E-mail: zhou1168@purdue.edu.

• Voicu Popescu is with Purdue University. E-mail: popescu@purdue.edu.

Manuscript received xx xxx. 201x; accepted xx xxx. 201x. Date of Publication xx xxx. 201x; date of current version xx xxx. 201x. For information on obtaining reprints of this article, please send e-mail to: reprints@ieee.org. Digital Object Identifier: xx.xxxx/TVCG.201x.xxxxxxx

¹<https://www.meta.com/quest/quest-3>

²<https://www.vive.com/us>

³<https://www.apple.com/apple-vision-pro>

In this paper we investigate the effect of the realism of the user’s surroundings and of the user’s hand on haptic redirection. We put forth two competing hypotheses. On one hand, it could be that the user’s familiarity with their actual physical surroundings and their actual hand makes the redirection manipulations more conspicuous, increasing the user’s acuity at detecting them. On the other hand, it could be that when the user sees their own hand and their actual physical surroundings, any redirection manipulation becomes less plausible, lowering the user’s guard, and allowing for more sizable manipulations to go undetected. We have conducted an IRB-approved user study ($N = 30$) in which participants saw either a virtual environment or their actual physical surroundings, i.e., VR scene vs. MR scene, and saw their hand rendered either with a generic 3D computer graphics model or using a 2D video sprite of their hand, i.e., VR hand vs. MR hand (Fig. 1). We used a two-alternative forced choice (2AFC) design asking participants to detect hand redirections that bridged real to virtual offsets of different sizes. The results show that participants were *not* more sensitive to redirection when they saw their actual hand in their actual physical surroundings. To the contrary, the results even bring preliminary evidence that users might be *less* sensitive to redirection in MR than in VR, which opens the door to haptic redirection in MR. We note that our comparison between VR and MR is affected by confounding factors such as hand representation differences, i.e., 3D in VR and 2D in MR, and such as a slightly larger latency in MR compared to VR. Although our results cannot be directly extrapolated to *perfect* MR, they do inform on the difference between the VR and MR redirection implementations possible at this time. We also refer the reader to the video accompanying our paper.

In summary, our paper makes the following contributions: (1) A system for hand redirection in MR that changes the position where the user sees their hand in video passthrough mode. (2) A user study ($N = 30$) with four conditions that investigates differences in hand redirection detection between VR and MR hand representations and VR and MR environments.

2 RELATED WORKS

We review prior work on hand redirection techniques (Sec. 2.1), practical applications (Sec. 2.2), and effects (Sec. 2.3), establishing the basis for our study of hand redirection across VR and MR.

2.1 Hand Redirection Techniques

Zenner et al. [62] categorize redirection techniques into three types: body warping, world warping, and hybrid warping. In this paper, we focus on hand warping, which modifies the virtual hand’s position relative to the physical hand either continuously or instantaneously, while minimizing perceptual discrepancies. The main idea is to help extend the human ability to interact with virtual objects with haptic feedback without breaking user immersion.

Prior work has explored a range of hand redirection techniques. Azmandian et al. [1] proposed haptic retargeting through body manipulation to dynamically align a single physical prop with multiple virtual objects. Cheng et al. [11] introduced Sparse Haptic Proxy, using continuous redirection guided by eye gaze and hand motion to steer users toward shared proxy surfaces. Han et al. [25] compared static translational offsets and interpolated movement, finding the former more effective in high-level mismatched reach tasks. Benda et al. [7] studied fixed positional offsets in six directions (left, right, close, far, up, down), revealing direction-dependent detection thresholds. Hartfill et al. [26] investigated motion scaling via decelerated hand movement, showing that detection thresholds varied significantly by movement direction.

Building on these prior works, our study explores hand redirection along both lateral (left-right) and depth (near-far) directions on a tabletop surface. We apply consistent redirection stimuli using a predefined set of spatial offsets and continuously compute the redirected hand position along the specified axis.

2.2 Hand Redirection Applications

Hand redirection has been applied across diverse VR applications to enhance interaction efficiency, comfort, and system adaptability. Gonzalez et al. [22] proposed REACH+, a dynamic redirection framework that improves timing accuracy and realism for encounter-type haptic devices by predicting hand arrival time and adjusting contact points accordingly. Matthews et al. [35, 36] investigated remapped hand techniques to improve alignment between visual and physical interaction spaces. Montano-Murillo et al. [40] introduced Erg-O, a strategy that reduces fatigue by retargeting interaction points to more ergonomic physical locations using spatial partitioning and optimization. Feuchtnauer and Müller [18] developed Ownershift, which gradually shifts the virtual hand space during prolonged overhead interactions, allowing the physical hand to move to a more comfortable position while maintaining ownership. Xiong et al. [59] applied hand redirection to VR-based upper limb rehabilitation, showing that patients tolerate hand discrepancies well and find the technique motivating. Ogawa et al. [43] proposed Redirected Drawing, using translation gain to enlarge the perceived drawing space in VR, particularly effective with pen-based input on physical surfaces.

This prior work highlights the potential of hand redirection in VR, showcasing its adaptability across domains such as haptics, ergonomics, rehabilitation, and creative interaction. Building on these insights, we see promising opportunities to migrate hand redirection into MR, a space where users engage simultaneously with both physical and virtual worlds. MR not only preserves the illusion of seamless interaction but also opens up possibilities for manipulating real-world objects in intuitive and almost magical ways.

2.3 Perceptual Effects on Hand Redirection

Various factors influence the noticeability and detectability of hand redirection in virtual environments. Avatar appearance is an important one, due to the visual dominance of humans [10]. Ogawa et al. [45] found that realistic hand avatars led to a 31.3% higher detection thresholds compared to abstract hand representations, suggesting that stronger body ownership and greater proprioceptive drift contribute to reduced sensitivity to remapping. Hartfill et al. [27] further explored avatar realism and dexterity, showing that while embodiment varied across different hand models, detection thresholds remained largely unaffected. Notably, both studies used generic 3D hands with uniform skin tone for their realistic representations, leaving the effect of photorealistic hands unexplored—a gap our work addresses.

A series of studies by Ban et al. [2–5] introduced visual-only pseudo-haptic manipulation, showing that deforming the real-time image of a user’s hand can modulate perceptions of edge location [2], curvature [3], object size [4], and stiffness [5], and without requiring physical force feedback. Unlike the finger-level deformations [4, 5] that preserve visuo-tactile congruence and are conducted using a stereoscopic video see-through system with a monitor and webcams, our work applies hand-level redirection to investigate how avatar and scene realism affect redirection detectability, and is conducted in an MR HMD environment.

Beyond avatar appearance, recent studies have examined perceptual, sensory, and contextual factors influencing redirection. Zenner et al. [61, 65] and Groth et al. [23] showed that natural interruptions like blinks and saccades can mask hand redirection. Ponton et al. [46] found that maintaining avatar continuity through arm stretching enhances proprioception, embodiment, and performance, while Feick et al. [15] reported that more complete avatars improve embodiment with minimal effect on detectability. Ogawa et al. [44] demonstrated that noisy tendon electrical stimulation reduces proprioceptive reliability and alters detection thresholds without impacting embodiment or presence. Tanaka et al. [52] showed that redirection during motion replays increases JNDs, as users tend to underestimate replayed displacement.

Recent work by Venkatakrishnan et al. [54, 55] emphasized the value of avatarized hands in near-field AR and MR settings, showing that visually enhanced hand representations improve task performance and usability. These results reinforce the hypothesis that avatar realism plays a key role in hand-based interaction quality—particularly relevant in MR contexts where both real and virtual elements co-exist.

While most studies focus on fully virtual environments, hand redirection in MR remains underexplored. Matthews et al. [34] proposed an MR redirection method using video inpainting to remove the physical hand and target objects, but residual artifacts and lack of perceptual validation highlight the need for further investigation into redirection detectability in MR.

3 HAND REDIRECTION IN MIXED REALITY

Hand redirection in VR environments has been extensively studied [1, 26, 64, 67]. Implementing hand redirection in VR benefits from knowing the geometry and appearance of the scene and of the user’s virtual hand, which allows displacing the hand to a different position and rendering it in the virtual scene to achieve the hand redirection effect. Hand redirection in MR is more challenging.

3.1 Challenges and Approach

Hand redirection in MR is more challenging because one has to manipulate the user’s view of the real world. Hand redirection in MR implies addressing the following three challenges: (1) *Hand segmentation*, to isolate the user’s hand in their view of the real world; (2) *Hand deletion*, to remove the user’s hand from their view of the real world; and (3) *Hand re-rendering*, to show the user’s hand in a different position, within the user’s view of the real world.

All three steps must be performed in real time, for each frame, avoiding latency that is known to induce cybersickness in immersive visualization [51]. Furthermore, the visual quality has to be high to sustain the user’s illusion that they continue to see their actual hand in their actual physical surroundings. The first two steps amount to a challenging diminished reality [42] exercise, where the output view, i.e., the user’s first person view, is dynamic, where the object to be removed, i.e., the user’s hand, has complex geometry that deforms non-rigidly, and where the background over which the user sees their hand can also be dynamic. The third step requires real-time photorealistic 3D modeling of the user’s hand for it to be rendered at a different position.

MR headsets adopt one of two technologies. Optical see-through headsets (e.g., Microsoft’s now discontinued HoloLens⁴) let the user see the real world directly, through a transparent visor. Optical see-through has important challenges such as lack of support for true opacity, which complicates deleting the hand from the user’s view, and such as a limited active field of view, which restricts redirection to a small subset of the user’s field of view. Video passthrough headsets capture the real world with cameras whose feeds are shown on the headset displays. Video passthrough headsets are more suitable for hand redirection in MR because they simplify the manipulation of the user’s view of the real world: the hand can be deleted effectively by inpainting, through pixel manipulations on the opaque conventional displays catering to the user’s eyes, bypassing the see-through challenge of having to mask off the hand by rendering a transparent background layer on top of it. Video passthrough technology has challenges of its own, including the offset between the cameras and the user eyes, which is significant for objects close to the user’s eyes, and which is addressed imperfectly through distortions. We develop and investigate MR hand redirection for video passthrough headsets, which is, at least for now, the prevalent MR technology.

Computer graphics research advances such as neural radiance fields (NeRF [39]) and 3D Gaussian Splatting [32] now allow for the photorealistic interactive rendering of real-world scenes from novel viewpoints. Recently, researchers have also demonstrated support for scenes with moving objects [29, 58], and even for interactive, physics-based modifications of the scene [30]. However, these approaches rely on building offline comprehensive implicit or explicit representations of the 3D scene and are therefore not yet suitable for real-time applications such as hand redirection in MR.

In order to answer our central research question of whether and how much hand redirection can go undetected by the user in MR, we have developed an MR hand redirection pipeline based on several simplifying assumptions. One is that there is sufficient contrast between

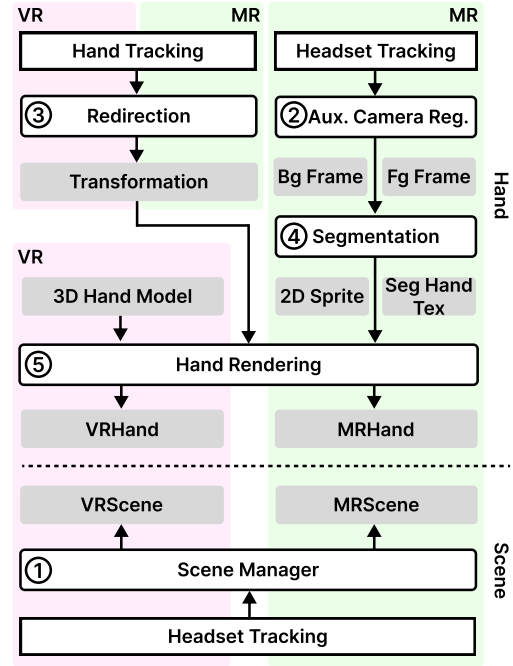


Fig. 2: VR and MR hand redirection system overview: VR components in pink, MR in green, and input and output data in grey.

the workspace and the hand, for robust hand segmentation. Another is that the workspace can be captured and rendered with a simple textured mesh, to allow deleting the user’s hand by rendering the workspace on top of the passthrough video frame. A third assumption is that redirection implies a limited displacement of the user’s hand. For example, it is reasonable to assume that if the user reaches into the workspace with a palm-down index-pointing hand gesture, redirection will *not* be asked to retract the pointing finger or to flip the hand for a palm-up gesture. Examples of typical redirections are to displace the hand to the left or to the right, or closer or farther. For such displacements, a real-time video sprite model of the hand is sufficient. The video sprite captures the appearance of the hand photorealistically, making it immediately recognizable by the user as their own hand, it preserves visual fidelity even after redirection displacements, and it implies only a modest capturing and rendering cost, making the approach tractable on MR headsets.

3.2 MR Hand Redirection System

Our VR and MR hand redirection pipeline is shown in Fig. 2.

The **Scene Manager** (① in Fig. 2) aligns the virtual and physical workspaces. In VR, the alignment is needed for the physical workspace to provide haptic feedback when the user touches the virtual workspace. In MR, the alignment is needed to allow deleting the user’s hand that is visible over the workspace, by rendering the virtual workspace on top of the video passthrough frame. Workspace alignment is done with the handheld controller, either once per session, or just once for each workspace by leveraging saved scene anchors⁵. In our experiments the workspace is a rectangular table (Fig. 1). In MR, a reference background frame is acquired for hand segmentation.

Auxiliary Camera Registration (② in Fig. 2). To support hand redirection in MR, the user’s hand and/or the user’s physical surroundings have to be acquired from the user’s perspective. The eye cameras built into the headset for video passthrough support are ideal for fulfilling this role. However, many MR headsets do not give developers access to the passthrough video feed, or do so with long latency precluding real-time hand interaction. At the request of developers, MR headset manufacturers, such as Meta, are in the process of exposing the video

⁴<https://learn.microsoft.com/en-us/hololens>

⁵<https://developers.meta.com/horizon/documentation/unity/unity-scene-overview>

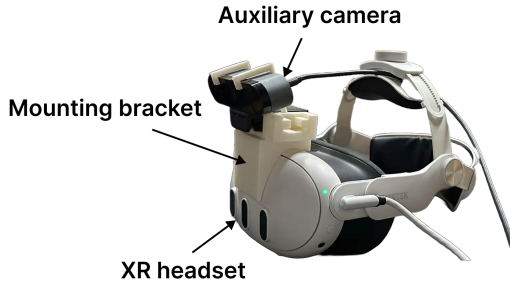


Fig. 3: XR headset with attached auxiliary camera for the low-latency capture of real-world frames.

passthrough feeds to developers for direct access. For now, like other researchers [16, 17], we overcome this barrier by attaching an auxiliary camera to the headset using a custom 3D printed bracket (Fig. 3). Both the camera and the headset are connected to a workstation. The auxiliary camera is fixed with respect to the headset, and its constant pose relative to the headset (virtual world) was calibrated with a conventional approach involving a black-and-white checkerboard [8]. This calibration registers the auxiliary camera to the scene as the user moves their head, providing frames that approximate the user’s view of their hand and physical surroundings.

Redirection (③ in Fig. 2). We rely on the hand tracking provided by the headset. The redirection module prescribes the displacement between where the user’s physical hand is and where the user sees their hand in VR or MR. The hand redirection module is based on the *incremental body warping algorithm* by Azmandian et al. [1], which gradually shifts the virtual hand for the physical hand to align with a physical target. Given the physical hand position W_0 when redirection begins, i.e., the activation position, the desired physical hand position W_T at the end of redirection, i.e., the physical target position, and the current hand position P_H , the *warping ratio* α is defined with the following equation.

$$\alpha = \max \left(0, \min \left(1, \frac{(W_T - W_0) \cdot (P_H - W_0)}{\|W_T - W_0\|^2} \right) \right)$$

The warping ratio is used to interpolate between the real and virtual targets, producing a redirected hand position. Inspired by the HaRT framework [62], we compute a transformation matrix that maps the physical to the redirected hand position, which is passed to the Hand Rendering module for rendering. This modular approach decouples redirection logic from environment-specific rendering, supporting consistent behavior across VR and MR setups.

Segmentation (④ in Fig. 2). We segment the user’s hand from the auxiliary camera frame through a background subtraction fragment shader, leveraging the reference workspace frame acquired during scene initialization.



Fig. 4: VR (left) and MR (right) hand rendering.

Hand Rendering (⑤ in Fig. 2). The Hand Rendering module is responsible for modeling and displaying the redirected hand according to the selected environment and redirection parameters. It takes as input the redirection transformation and the hand representation, applying the transformation in the vertex shader to produce the final rendering.

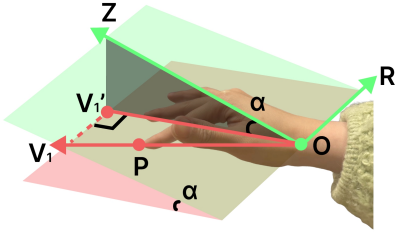


Fig. 5: MR hand alignment correction using the tip of the index finder as the contact point. Notations were used by Alg. 1.

Algorithm 1 Visual-Tactile Alignment for MR Hand

Input: With the notations from Fig. 5: Index finger tip P , wrist O , forward direction \overrightarrow{OZ} , with $\overrightarrow{OR} \perp \overrightarrow{OzV'_1}$

Output: Updated local rotate angle α for the XR hand

- ```

1: $\overrightarrow{OV'_1} \leftarrow P - O$ ▷ get direction from O to P
2: $\overrightarrow{OV'_1} \leftarrow \overrightarrow{OV'_1} - \overrightarrow{OR}(\overrightarrow{OV'_1} \cdot \overrightarrow{OR})$ ▷ project $\overrightarrow{OV'_1}$ onto $P_{OzV'_1}$
3: $\alpha \leftarrow \arccos((\overrightarrow{OZ}/\|\overrightarrow{OZ}\|) \cdot (\overrightarrow{OV'_1}/\|\overrightarrow{OV'_1}\|))$ ▷ compute local rotation angle

```

For the VR hand mode, the hand is represented as a 3D skinned mesh rigged to the OVR Hand Skeleton<sup>6</sup>, see Fig. 4, left. The mesh includes pre-defined physically-based materials and it is scaled to the user’s approximate hand size during session initialization. For the MR hand mode, the hand is represented as a real-time 2D video sprite that reflects the user’s real hand appearance. The sprite is generated by projectively texture mapping the segmented auxiliary camera frame onto a 3D rectangle. The size of the MR hand sprite is dynamically determined using a headset provided hand scale factor<sup>7</sup> and 3D axis-aligned bounding box, allowing the sprite to approximate the user’s actual hand size from a first-person perspective, see Fig. 4, right.

One challenge in rendering the MR hand lies in maintaining accurate visual-tactile alignment, particularly when the user’s finger touches the table surface, the virtual (visual) and physical (tactile) contacts have to be synchronized. In an initial implementation, we applied the wrist pose to the entire 2D sprite, which resulted in a visual-tactile misalignment. To address this, we compute the sprite orientation to align the tip of the index finger with the physical surface at the moment of impact, as shown in Alg. 1 and Fig. 5. Furthermore, to account for minor but non-negligible hand tracking errors, the MR hand sprite is rendered with depth testing disabled to avoid the visual artifact of the hand sinking into the table.

This approach to hand rendering ensures a consistent visual feedback across conditions, enabling controlled and comparable evaluation of hand redirection between VR and MR environments.

## 4 USER STUDY

We conducted an IRB-approved user study to compare four conditions defined by all  $\{\text{VR}, \text{MR}\} \times \{\text{scene}, \text{hand}\}$  combinations. The goal was to investigate the influence of the MR scene and hand visual realism on redirection detectability.

### 4.1 Design

The study employed a within-subject design to compare four conditions: VR hand and VR scene (VRH\_VRS), VR hand and MR scene (VRH\_MRS), MR hand and VR scene (MRH\_VRS), and MR hand and MR scene (MRH\_MRS). To mitigate learning effects and order bias, the presentation order of the conditions was counterbalanced across participants using a Latin Square design [20].

<sup>6</sup>[https://developers.meta.com/horizon/reference/unity/v64/class\\_o\\_v\\_r\\_skeleton](https://developers.meta.com/horizon/reference/unity/v64/class_o_v_r_skeleton)

<sup>7</sup>[https://developers.meta.com/horizon/reference/unity/v67/class\\_o\\_v\\_r\\_hand](https://developers.meta.com/horizon/reference/unity/v67/class_o_v_r_hand)

The study used a 2AFC design, which is the golden standard in detection threshold research, avoiding the bias of designs based on yes/no questions [47]. For each trial, the participant was asked to touch with their index finger a virtual target, to retract their hand, and then to touch a second virtual target. In one of the touches hand redirection was applied, and in the other touch no redirection was applied. After each trial, the participant was asked to indicate in which of the two touches their hand did not move as expected, and detection thresholds were derived from the response correctness rate data.

## 4.2 Hand Redirection Latency

Tab. 1 shows CPU and GPU frame times across 600 frames for the four study conditions. All conditions sustained frame rates above 60 FPS (approximately 90 FPS), ensuring a comfortable XR experience [60]. CPU times dominate GPU times, but differences across conditions were minimal (e.g., 0.04 ms more for the MR hand compared to the VR hand in the MR scene). This latency is below the perceptual threshold for detecting visual delay differences, typically within 10–15 ms [24], making it unlikely participants noticed it.

Table 1: CPU frame time statistics and GPU average frame time over 600 sampled frames (all values in ms except FPS).

| Cond.   | Mean  | Min  | Max   | Std  | FPS   | GPU  |
|---------|-------|------|-------|------|-------|------|
| MRH_MRS | 11.20 | 4.29 | 39.51 | 2.10 | 89.31 | 2.67 |
| VRH_MRS | 11.16 | 4.35 | 36.84 | 2.02 | 89.62 | 2.55 |
| MRH_VRS | 11.13 | 4.67 | 26.96 | 2.00 | 89.81 | 2.63 |
| VRH_VRS | 11.13 | 4.41 | 19.31 | 1.84 | 89.88 | 2.55 |

## 4.3 Participants

We recruited  $N = 30$  participants from our institution’s human subject pool. The average age of the participants is 22.5 (SD = 4.26), ranging from 18 to 37, with 11 self-identifying as female and 19 as male. Among them, 27 were right-handed, 2 were left-handed, and 1 was ambidextrous. Regarding prior VR experience, 4 participants had never used VR before, 7 had tried it once, 15 use VR occasionally, and 4 use it frequently. All participants had normal or corrected-to-normal vision. An adjustable head strap was used with the headset to ensure comfort and stability during the task.

## 4.4 Procedure

Upon arrival at the experiment site, consenting participants completed a demographics questionnaire, they were seated at the experimental table, and the experimenter assisted them in putting on the headset. Each participant completed all four experimental conditions in a counterbalanced order. At the beginning of each condition, instructions were shown inside the headset, guiding participants through an initial calibration process. This included adjusting the virtual table height using the bottom of their dominant-hand controller. For the two MR hand conditions, participants were also instructed to capture a background image of the empty table for hand segmentation purposes. After calibration, participants performed a brief (approx. 5 min) training session in which the experimenter explained how to use the index fingertip of their dominant hand to touch a virtual green dot. Participants were instructed to carefully observe both touches in each trial and to identify the one that felt inconsistent with their actual hand movement. They were encouraged to ask questions until they felt comfortable with the task procedure. Once participants confirmed their understanding of the task, data collection commenced.

A participant completed multiple trials per condition. We used two workspace points, A and B, as physical targets to which redirection guided the user’s physical hand. The use of two physical targets is needed to avoid that the user memorize the position of the physical target when no redirection is applied. Offsets were applied along the left-right (X) and the near-far (Y) directions in the table plane. We used 8 X and 8 Y offsets, in the -12 cm to 12 cm range, with 3 cm

increments, and a 0 cm offset (no offset), for a total of 17 offsets. Each offset was tested twice, once with the redirected touch occurring first, and once with it occurring second. A participant completed 68 trials in each condition: 2 physical targets  $\times$  17 offsets  $\times$  2 repetitions. The order of offset values and redirection targets was randomized to avoid predictability and learning effects.

The selection of the number of physical targets and of their locations is guided by competing concerns. On one hand, we wanted to test locations within the user’s reach in a 2D desktop-sized user workspace. On the other hand, we wanted to avoid user fatigue, which can corrupt the data acquired. We compromised by selecting two target locations, one near one far, one left one right. For a 2AFC design like ours, the offset range always starts at 0 and then has to extend sufficiently to yield consistently correct detections at the far end. The 12 cm far end was selected through experiments that revealed that at 12 cm redirection is quite noticeable. Our results do confirm that the range did indeed bracket the detectability thresholds of participants (Sec. 4.7.1). The resolution with which the range of offsets is investigated is also dictated by competing concerns. One concern is again participant fatigue. The other is to ensure that there are sufficient measurement points as the correctness rate flips from 50% to 100%. Our results do confirm (Sec. 4.7.1) that the 3 cm step samples the sigmoid adequately.

After each condition, participants filled out three questionnaires: the System Usability Scale (SUS) [9], the Simulator Sickness Questionnaire (SSQ) [31], and a custom User Experience Questionnaire (UEQ). Participants were allowed to take breaks between conditions. The total duration of the study was approximately 90 minutes per participant, and participants were compensated with a \$40 gift card for their time. Participants were informed that they should withdraw from the study at any time if they experienced discomfort, without forfeiting their compensation.

## 4.5 Implementation

The MR and VR redirection system (Sec. 3.2) was developed in Unity<sup>8</sup> (version 2022.3.17f1), integrated with the Meta XR All-in-One SDK<sup>9</sup> (version 64.0.0). The study was conducted on a Windows 11 PC equipped with an Intel Core i9-13900 CPU, 32 GB of RAM, and an NVIDIA GeForce RTX 4080 GPU. Participants used a Meta Quest 3 headset, paired with two handheld controllers. A Logitech Brio webcam<sup>10</sup> was mounted on top of the headset to capture video frames at a resolution of 1280  $\times$  720 with a 90° diagonal field of view, see Fig. 1, left, and Fig. 3. Both the headset and the webcam were connected to the PC via USB Type-C cables. Participants were seated in front of a table (see the supplementary video) measuring 1.53 m in length, 0.76 m in width, and 0.73 m in height, covered with a black cloth to guarantee robust segmentation, avoiding the confounding factors of segmentation artifacts.

## 4.6 Data Collection and Analysis

We collected both objective and subjective metrics to evaluate participants’ performance and experience across conditions.

**Descriptive and inferential statistics.** We used violin plots with embedded boxplots to visualize the distribution of correctness and SUS scores. These plots illustrate data density, along with key summary statistics including the median, interquartile range (IQR), mean, and outliers. SSQ scores were shown with standard boxplots, and UEQ responses were presented as stacked bar plots to depict the five-point Likert scale distribution. For significant results, we quantified effect size using Cohen’s dz for paired t-tests [13], and Cohen’s r for Wilcoxon’s tests [19], and we used the effect sizes to estimate the statistical power provided by our number of participants for each test.

**Objective Metrics.** We recorded the answer correctness for each trial, and the data was analyzed by: (1) estimating detection thresholds

<sup>8</sup><https://unity.com>

<sup>9</sup><https://developers.meta.com/horizon/downloads/package/meta-xr-sdk-all-in-one-upm>

<sup>10</sup><https://www.logitech.com/en-us/products/webcams/brio-4k-hdr-webcam.html>

via psychometric modeling, (2) evaluating the overall correctness per condition, and (3) analyzing correctness rates at each offset across conditions.

*Detection threshold computation.* To model detection performance across redirection offsets, we fit a sigmoid psychometric function of the form:

$$\Sigma(x; a, b, \delta) = 0.5 + \frac{0.5}{1 + e^{\delta b(x-a)}}$$

where  $x$  is the redirection offset,  $a$  is the detection threshold (i.e., the offset at which participants reached 75% accuracy),  $b$  controls the slope of the curve (reflecting sensitivity), and  $\delta \in \{-1, 1\}$  indicates the direction of redirection—negative for rightward (increasing sigmoid), positive for leftward (decreasing sigmoid). Separate sigmoid fits were applied to leftward and rightward data using constrained nonlinear least squares.

*Overall correctness analysis.* After confirming both data normality, via the Shapiro-Wilk test [49], and sphericity, via Mauchly's test [37], we applied a repeated-measures ANOVA to evaluate differences between conditions, followed by paired t-tests for  $\times 6$  Bonferroni-corrected posthoc pairwise comparisons.

*Per offset correctness analysis.* For (3), correctness at each individual offset was treated as a binary variable (True/False). We used Cochran's Q test [12] to assess differences across the four conditions. If significance was found, we conducted pairwise comparisons using McNemar's test [38] with Bonferroni correction.

**Subjective Metrics.** Subjective metrics included standard SUS and SSQ questionnaires, analyzed using prescribed methods and compared across conditions. Since SUS scores were not normally distributed, we used the non-parametric Friedman test [21] to assess overall differences among conditions, followed by Wilcoxon signed-rank test [57] for post hoc pairwise comparisons.

We also developed a custom user experience questionnaire (UEQ) with seven items designed to assess user preferences and perceived realism, using a five-point Likert scale (1: “strongly disagree” to 5: “strongly agree”). The questions were: **Q1**, “In some trials it was *obvious* in which of the two touches the hand seen in the headset was moving differently than my real hand”; **Q2**, “In some trials it was *impossible* to tell in which of the two touches the hand seen in the headset was moving differently than my real hand”; **Q3**, “I was never confident; I guessed all the time”; **Q4**, “I always felt pretty sure of my answer”; **Q5**, “I felt like the hand I saw in the headset was a live video of my own hand”; **Q6**, “Sometimes the hand I saw in the headset touched the dot before or after I felt the contact with the table”; and **Q7**, “I am fine with the hand seen in the headset not moving like my real hand”.

Since UEQ scores were not normally distributed, we used the Friedman test to analyze the overall differences among conditions.

## 4.7 Results and Discussion

To ensure data reliability, we filtered out inattentive trials using the Spearman correlation test [50]. For each participant and condition we calculated the correlation between offset magnitude and correctness across the four redirection groups AX, AY, BX, and BY, where the first letter indicates the physical target, and the second the displacement direction. Participants with more than one subgroup showing a negative trend (correlation  $< -0.1$ ), indicating declining performance with increasing offset, were excluded from that condition. The filtering removed the data of 2, 3, 1, and 2 participants from each condition. This left the data of 28 participants in the MRH\_MRS, of 27 in the MRH\_VRS, of 29 in the VRH\_MRS, and of 28 in the VRH\_VRS conditions, which was used to compute per condition detection thresholds. Furthermore, 24 participants had valid data across all four conditions, and their data was used for statistical comparisons across conditions.

### 4.7.1 Detection Thresholds

The detection threshold computation is shown in Fig. 6 and the thresholds are shown in Tab. 2, for each redirection group, in rows 1-4. For our 2AFC design, the sigmoid function value  $f(x) = 0.5$  indicates the

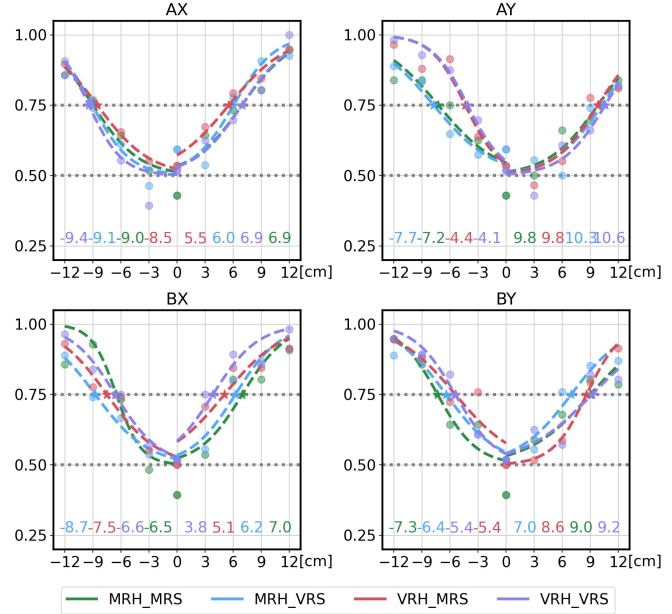


Fig. 6: Psychometric sigmoid fits for the computation of detection thresholds for four conditions and four redirection groups. A group is defined by a physical redirection target A or B, and by an offset axis X or Y. In each subplot, the x-axis indicates redirection offset in cm.

point of subjective equality (PSE) [47], while  $f(x) = 0.75$  defines the correct response rate threshold for detection.

**MR hand vs. VR hand.** Notable differences in detection thresholds (DTs) were observed in three redirection groups: AY with near offsets, i.e., towards the user (-12 to 0 cm), BY with near offsets, and BX with right offsets (0 to 12 cm). For all three groups, the MR hand conditions (MRH\_MRS and MRH\_VRS) yielded larger DTs than their VR hand counterparts (VRH\_MRS and VRH\_VRS). Specifically, for AY near, the average DT for the two MR hand conditions was -7.45 cm, compared to -4.25 cm for the VR hand conditions. For BY near, the MR hand conditions averaged -6.85 cm, vs. -5.4 cm for the VR hand conditions. In BX right, MR hand conditions averaged 6.6 cm, vs. 4.45 cm for the VR hand conditions.

**MR scene vs. VR scene.** In contrast, differences between scene types were smaller. Two groups showed slight separation: AX with left offsets and AY with far offsets. In AX left, MR scene conditions averaged -8.75 cm, while the VR scene conditions averaged -9.25 cm. In AY far, MR scene conditions averaged 9.8 cm, compared to 10.45 cm for the VR scene conditions.

Table 2: Detection thresholds in cm. Columns: condition and offset direction (L/N denote negative offsets—Left for X and Near for Y; R/F denote positive offsets—Right for X and Far for Y). Rows 1-4: four redirection groups {A, B}  $\times$  {X, Y}. Rows 5-9: average detection thresholds for each physical target {A, B}, offset direction {X, Y}, and condition (Overall).

| Cond.   | MRH_MRS |     | MRH_VRS |      | VRH_MRS |     | VRH_VRS |      |
|---------|---------|-----|---------|------|---------|-----|---------|------|
|         | L/N     | R/F | L/N     | R/F  | L/N     | R/F | L/N     | R/F  |
| AX      | -9.0    | 6.9 | -9.1    | 6.0  | -8.5    | 5.5 | -9.4    | 6.9  |
| AY      | -7.2    | 9.8 | -7.7    | 10.3 | -4.4    | 9.8 | -4.1    | 10.6 |
| BX      | -6.5    | 7.0 | -8.7    | 6.2  | -7.5    | 5.1 | -6.6    | 3.8  |
| BY      | -7.3    | 9.0 | -6.4    | 7.0  | -5.4    | 8.6 | -5.4    | 9.2  |
| A       | 8.23    |     | 8.28    |      | 7.05    |     | 7.75    |      |
| B       | 7.45    |     | 7.08    |      | 6.65    |     | 6.25    |      |
| X       | 7.35    |     | 7.50    |      | 6.65    |     | 6.68    |      |
| Y       | 8.33    |     | 7.85    |      | 7.05    |     | 7.33    |      |
| Overall | 7.84    |     | 7.68    |      | 6.85    |     | 7.00    |      |

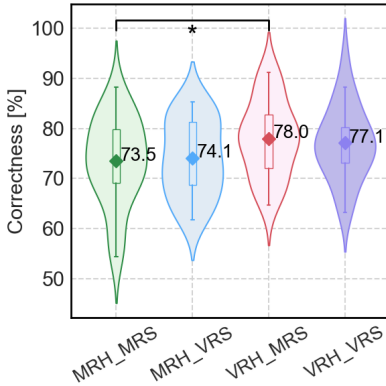


Fig. 7: Violin plots of the overall correctness across the four conditions. Means are marked with diamonds and provided numerically. The asterisk indicates a significant difference.

**Average detection thresholds.** Tab. 2 also gives in Rows 5-9 the average absolute DTs for each redirection target A and B, for each offset direction X and Y, and overall. For all five of these averages, MR hand consistently exhibited higher DTs than VR hand.

#### 4.7.2 Analysis of Response Correctness

To validate the trends observed in the detection threshold analysis, we conducted statistical tests on the correctness rate of the participant responses. We analyzed correctness over all offsets, as well as over individual offsets. The overall and individual correctness was compared across the four conditions.

**Overall Correctness** was computed for each participant and each condition as the proportion of correct responses out of the total number of trials in a condition (i.e., 68). The results are shown in Fig. 7 and Tab. 3. The data satisfied the normality (Shapiro-Wilk test,  $p > 0.05$ ) and sphericity (Mauchly's test,  $p > 0.05$ ) assumptions. A repeated measures ANOVA revealed a significant difference among the four conditions in overall correctness ( $F(3, 69) = 4.27$ ,  $p = 0.008$ ). We performed a posthoc pairwise analysis using paired t-tests, with a  $\times 6$  Bonferroni correction to account for the 6 pairs of conditions. The overall correctness in the MRH\_MRS condition was significantly lower than in the VRH\_MRS condition ( $t(23) = -3.13$ ,  $p \times 6 = 0.0285$ ), as highlighted in yellow in Tab. 3. The post-hoc statistical power analysis reveals that the test is underpowered and more participants are needed to strengthen the confidence in the significance of this difference. No other pairwise differences reached statistical significance after correction. This suggests that in video passthrough mode, when the user sees their physical surroundings (MR scene), using a realistic depiction of the participant's hand significantly reduces the participants' ability to detect hand redirection compared to using a generic VR hand. As illustrated in Fig. 7, the average overall correctness for MR hand conditions (MRH\_MRS = 73.5%, MRH\_VRS = 74.1%) was consistently lower than for VR hand conditions (VRH\_MRS = 78.0%, VRH\_VRS = 77.1%).

**Individual Correctness** was analyzed as a dichotomous variable (True/False) for each trial, across all combinations of redirection target

Table 3: Post-hoc correctness comparisons between condition pairs. Displayed  $p$ -values are Bonferroni-corrected ( $\times 6$ ) for readability against  $\alpha = 0.05$ ; statistical power is computed using the corrected threshold  $\alpha = 0.0083$ .

| Post-hoc Comparisons | t-value | p-value | d    | Power |
|----------------------|---------|---------|------|-------|
| MRH_MRS vs. MRH_VRS  | -0.335  | >1.000  | 0.07 | 1.2%  |
| MRH_MRS vs. VRH_MRS  | -3.125  | 0.0285  | 0.64 | 60%   |
| MRH_MRS vs. VRH_VRS  | -1.969  | 0.367   | 0.40 | 21%   |
| MRH_VRS vs. VRH_MRS  | -2.555  | 0.106   | 0.52 | 39%   |
| MRH_VRS vs. VRH_VRS  | -2.629  | 0.090   | 0.54 | 42%   |
| VRH_MRS vs. VRH_VRS  | 0.658   | >1.000  | 0.13 | 2.2%  |

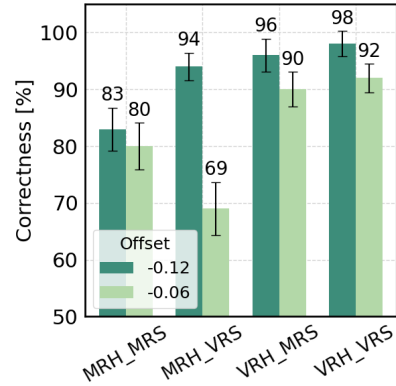


Fig. 8: Bar plot showing the mean correctness rates with scaled error bars for redirection detection at -6 cm and -12 cm offsets in the AY group across the four conditions.

(A or B), offset direction (X or Y), and magnitude. Since each participant completed two trials per condition, Cochran's Q test was used within each combination to evaluate whether there were significant differences in detection performance across the four conditions. If a significant difference was found, pairwise comparisons were performed using McNemar's test with Bonferroni correction.

Significant differences among the four conditions were observed in the AY group at offsets  $-0.12$  and  $-0.06$ ,  $\chi^2(3) = 9.67$ ,  $p = 0.0216$  and  $\chi^2(3) = 10.50$ ,  $p = 0.0148$  respectively. However, no pairwise comparisons were statistically significant after Bonferroni correction based on McNemar's test. Fig. 8 illustrates the mean correctness rates at AY for these two offsets. On average, the VR hand conditions (VRH\_MRS and VRH\_VRS) yielded higher detection correctness than the MR hand conditions (MRH\_MRS and MRH\_VRS).

#### 4.7.3 User Experience

The results of the custom user experience questionnaire (UEQ), with answers on a five-point Likert scale, are summarized in Fig. 9. A non-parametric Friedman test revealed no statistically significant differences across the four conditions for any of the seven questions (Q1–Q7). For analysis and discussion, we grouped the questions into five subjective categories: perceived detectability (Q1, Q2), confidence (Q3, Q4), hand realism (Q5), synchronization (Q6), and acceptability (Q7).

For *perceived detectability*, all conditions showed comparable responses: Q1 (MRH\_MRS = 4.3, MRH\_VRS = 4.2, VRH\_MRS = 4.4, VRH\_VRS = 4.1) and Q2 (3.9, 4.1, 4.2, 4.1), indicating that participants across all conditions found it similarly easy or difficult to detect redirection. In terms of *confidence*, MRH\_VRS showed slightly lower scores than the other conditions: Q3 (2.4, reverse-coded: "I was never confident; I guessed all the time") and Q4 (2.9: "I always felt pretty sure of my answer"). For *hand realism* (Q5), scores decreased in the order of MRH\_MRS (3.3), MRH\_VRS (3.1), VRH\_MRS (3.1), and VRH\_VRS (2.8), suggesting that participants perceived the MR hand as more visually realistic than the VR hand. Regarding *perceived synchronization between the visual and physical hand* (Q6), lower values indicate better synchronization. VRH\_VRS yielded the best score (3.3), followed by VRH\_MRS (3.6), MRH\_MRS (3.6), and MRH\_VRS (3.8), indicating slightly better haptic alignment in VR hand conditions. Finally, for *redirection acceptability* (Q7: "I am fine with the hand seen in the headset not moving like my real hand"), responses were similarly distributed across all conditions. On average, 11 out of 30 participants expressed acceptance, while 10 to 16 participants per condition indicated discomfort with the visual-proprioceptive mismatch.

#### 4.7.4 System Usability and Cybersickness

The SUS scores are shown in Fig. 10, left. According to established SUS interpretation guidelines [6], both MR hand conditions fall within the adjective label "OK", correspond to a letter grade of "C", and are classified under the "Marginal" acceptability range with a Net Promoter

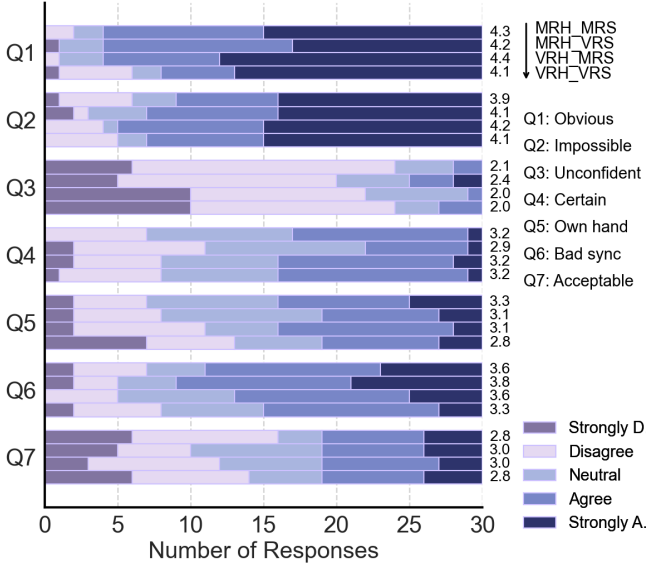


Fig. 9: Responses to the custom user experience questionnaire. Each bar shows the distribution from 30 participants, with conditions stacked top to bottom as indicated in the legend.

Score (NPS) rating of “Passive”. In contrast, the VR hand conditions received substantially higher ratings: VRH\_MRS corresponds to a grade of “B+”, and VRH\_VRS to “A−”, both falling within the adjective label “Good” and the “Acceptable” usability range. Notably, VRH\_VRS also reaches the highest NPS category of “Promoter”, indicating strong user satisfaction. As the SUS scores were not normally distributed, a Friedman test was conducted and revealed a significant difference among the four conditions ( $\chi^2(3) = 12.552, p = 0.006$ ). Post hoc comparisons (Tab. 4) indicated that MRH\_MRS was rated significantly lower than VRH\_MRS ( $Z = -72.5, p \times 6 = 0.017$ ). These results suggest participants had no clear preference for scene type (VR vs. MR) but preferred the VR hand over the MR hand.

The SSQ results are shown in Fig. 10, right. The average total scores (TS) were: MRH\_MRS = 15.46, MRH\_VRS = 17.08, VRH\_MRS = 14.71, and VRH\_VRS = 15.33. While the MR hand conditions showed slightly elevated oculomotor strain (e.g., O = 20.21 in MRH\_VRS), no statistically significant differences were observed among the four conditions. All total SSQ scores remained below the commonly cited discomfort threshold of 20 [14, 48], indicating low levels of cybersickness overall. This may be attributed to the stationary nature of the task, minimal visual motion, and frequent physical grounding during redirection interactions.

#### 4.8 Main Findings and Discussion

Overall, the study did not reveal strong statistically significant differences across conditions in either objective or subjective measures. Nonetheless, several patterns and observations provide useful insights into the applicability of hand redirection in MR environments.

**Detection Thresholds and Correctness.** Due to time constraints in our within-subject design, each redirection offset was tested only twice per participant, limiting the ability to estimate individual detection thresholds. To address this, we analyzed correctness at two levels: over-

Table 4: Wilcoxon test results for SUS pairwise comparisons.

| Post-hoc Comparisons | Z      | p-value | r    | Power |
|----------------------|--------|---------|------|-------|
| MRH_MRS vs. MRH_VRS  | -189.5 | >1.000  | 0.16 | 14%   |
| MRH_MRS vs. VRH_MRS  | -72.5  | 0.017   | 0.60 | 89%   |
| MRH_MRS vs. VRH_VRS  | -84.5  | 0.071   | 0.56 | 84%   |
| MRH_VRS vs. VRH_MRS  | -92.5  | 0.070   | 0.53 | 80%   |
| MRH_VRS vs. VRH_VRS  | -96.0  | 0.089   | 0.51 | 77%   |
| VRH_MRS vs. VRH_VRS  | -213.5 | >1.000  | 0.07 | 7.1%  |

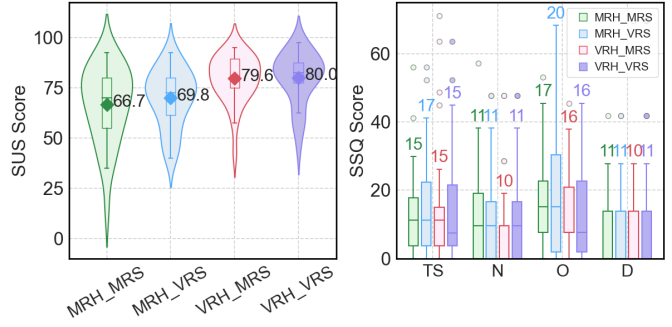


Fig. 10: Left: Violin plots of SUS scores by condition. Right: Boxplots of SSQ scores—Total (TS), Nausea (N), Oculomotor (O), and Disorientation (D)—with rounded means above whiskers.

all correctness (aggregated per condition) and individual correctness (per offset). While trends in the detection threshold data indicated that MR hand conditions tended to yield slightly higher thresholds than VR hand, these differences were not consistently supported by statistical tests.

Participants’ post-study feedback also aligned with their UEQ responses, with many stating that they perceived little to no difference across the four conditions when identifying redirection. This suggests that hand redirection can be reasonably applied in MR environments without significantly compromising the illusion. Interestingly, the data showed a trend toward *lower* detectability with MR hand, which is contrary to the expectation that MR, by revealing more of the physical world, might increase sensitivity to mismatches. A possible explanation of this trend is that participants tend to believe what they see more when the scene and the hand depiction match their physical surroundings and their own hand, compared to a VR scene and a VR hand. Participants harbor the implicit assumption that the realistically depicted hand and surroundings are tamper proof, and hence dismiss any secondary cue of possible tampering. This finding aligns with Ogawa et al. [45], who reported that more anthropomorphic hand avatars lead to higher redirection thresholds. Specifically, our results show elevated thresholds for the 2D photorealistic hand avatar. However, unlike their study, which found threshold differences primarily in the leftward (negative horizontal) direction, we observed slightly higher thresholds in the rightward direction (e.g., BX with offsets > 0). Additionally, our findings extend theirs by showing that the MR hand condition results in higher detection thresholds than the VR hand in the nearward direction (e.g., AY and BY with offsets < 0).

As discussed in Section 4.2, MR hand redirection incurs slight latency, which can act as a confounding factor hiding the redirection from user detection, so one cannot infer that the detection thresholds apply to an ideal MR redirection without latency. Latency is a delay in updating the user’s hand position, so it acts like a redirection vector  $r_l$  that is added to the (target) redirection vector  $r_t$ . In all cases,  $r_l$  is against the user’s hand motion, which is always from near to far, so  $r_l$  is always from far to near. On the other hand, we have applied redirection both left-right and near-far, so  $r_l$  is sometimes orthogonal to  $r_t$ , sometimes aligned and in the same direction with  $r_t$ , and sometimes aligned but in opposite direction with  $r_t$ . Consequently, any effects of latency average out when averaging trials with a variety of  $r_l$  directions, giving robustness to the measurements reported in rows A, B, X, Y, and Overall of Tab. 2.

**Subjective Experience.** Participants reported similar levels of perceived detectability across conditions in the UEQ (Q1, Q2), which contrasts with the objective results suggesting slightly higher detection thresholds for MR hand. Confidence ratings (Q3, Q4) were generally low across all conditions (e.g., Q3 means: 2.1 to 2.4; Q4 means: 2.9 to 3.2), indicating overall uncertainty in participants’ judgments, regardless of the condition. While MR hand received higher ratings for realism (Q5), it did not translate to perceived accuracy in synchronization (Q6), and its higher scores (reverse-coded) on Q6 may indicate

some limitations of the 2D MR hand in conveying tactile alignment with the physical environment. These results suggest that realism alone does not guarantee better perceptual fidelity or confidence.

In the post-study feedback, most participants reported no preference between the VR and MR scenes during the task, possibly because they did not perceive the environment as influencing task performance. Furthermore, many noted that although the 2D MR hand represented their real hand, they preferred the 3D VR hand due to its stronger depth cues. The experimenter observed that some users took longer to get comfortable using the 2D MR hand to touch the target during training. The MR hand also showed slightly poorer contact synchronization (Q6 in Fig. 9) compared to the VR hand, although the index finger collider was carefully matched in position and size between the two representations.

**System Usability and Cybersickness.** SUS scores showed a clear trend favoring VR hand over MR hand, with MR hand conditions rated as “Marginal” and VR hand conditions rated as “Good”. These results imply a user preference for VR hand representations. This points out that any remaining imperfection of the MR hand representation, such as occasional segmentation artifacts, incur a high usability penalty. In other words, despite simplifying assumptions embraced for MR hand representation robustness, our MR hand representation might not yet be completely out of an “own hand” uncanny valley. Importantly, SSQ scores across all conditions remained well below the commonly VR discomfort threshold, indicating that hand redirection tasks in MR do not induce significant cybersickness, supporting the feasibility of extending hand redirection to MR without adverse effects on user comfort.

## 5 CONCLUSIONS. LIMITATIONS. FUTURE WORK.

**Conclusions.** This paper presents a comparative investigation of hand redirection across VR and MR environments, with a particular focus on how scene context and hand representation influence detection thresholds, usability, and user perception. By implementing a modular redirection system supporting combinations of VR/MR hand and scene, and conducting a within-subject study across four experimental conditions, we contribute one of the first explorations of redirection in MR settings.

Consistent trends emerged across both objective and subjective metrics. MR hands generally yielded higher detection thresholds and lower correctness, suggesting reduced sensitivity to redirection. These results include the effects of factors that confound the comparison between the two conditions, such as latency, so our conclusions cannot be extrapolated to a comparison between VR and an *perfect* MR condition. Participants reported minimal perceived differences across conditions, and overall confidence in redirection detection remained low, reflecting the potential for VR and MR redirection to evade user detection. VR hands were rated as more usable and acceptable, while MR hands were perceived as more realistic. Cybersickness remained low across all conditions.

These findings suggest that hand redirection can be effectively extended to MR settings, opening new possibilities for redirected interaction where users see their own physical hand and environment without compromising the illusion. While VR hands remain effective, MR hands emerge as a viable—and potentially advantageous—alternative. Rather than replacing VR hands, MR hands expand the design space by allowing redirection techniques to be applied in more grounded, mixed-reality scenarios.

**Limitations.** Our study set out to measure and compare redirection thresholds in VR and MR. Implementing redirection in MR is challenging due to the difficulty of segmenting the user’s hand over a dynamic and complex environment, of rendering the user’s hand at a different location, and of filling in the frame pixels corresponding to the newly disoccluded background. The approximations introduced by the imperfect solutions to each of these problems translate into visual artifacts, and their non-negligible computational cost translates to latency, i.e., a delay in updating the user’s hand position as the user moves it. We have resorted to solutions to these problems that are robust and that imply a small computational cost, e.g., segmentation assuming a

favorable background and rendering hand as a 2D sprite that is both fast and avoids reconstruction artifacts. Nonetheless, we acknowledge that, although reduced, visual artifacts, such as a 2D MR hand vs. a 3D VR hand, and latency are present in the MR condition, acting like confounding factors when comparing to the VR condition. Despite these confounding factors, which preclude a comparison between VR and *perfect* MR redirection, we put forth that our study contributes valuable information nonetheless, as it compares VR to an MR approach that is possible now. As the ability to implement MR redirection advances, reducing or eliminating latency, and allowing for perfectly photorealistic 3D reconstruction and rendering of the user’s hand, the thresholds computed by our study will have to be updated.

Our study was constrained by practical limitations inherent to within-subject designs, particularly the need to manage overall session duration. Consequently, each redirection offset was tested only twice per participant, limiting the reliability of individual psychometric fits and contributing to variability in detection threshold estimates. Furthermore, the MR hand representation, rendered as a 2D sprite using real-time video textures was visually realistic, but lacked depth cues and full articulation, potentially affecting both perceived synchronization and redirection performance.

Our exploration of virtual environment influences is limited, particularly regarding lighting, which can impact user immersion [55]. While we applied consistent virtual lighting and adjusted hand shading to minimize its effect on interaction, physical-world lighting also plays a role in MR, where users see through to the real environment. Future work could incorporate more precise lighting configurations to improve visual consistency in MR scenes.

Robust MR redirection will ultimately depend on advances in photorealistic digital twins of users and environments. Key technical challenges include real-time 3D reconstruction, accurate hand and object tracking, segmentation, and visual inpainting. Overcoming these barriers is essential to enable seamless MR experiences where redirection remains perceptually plausible and unobtrusive.

**Future Work.** Future research should investigate denser sampling of redirection offsets and more trials per condition to enable finer-grained psychometric modeling. Enhancing MR hand realism and alignment remains a critical direction, where advanced rendering approaches—such as neural radiance fields [39], or 3D Gaussian Splatting [32]—could improve both hand and scene representations. Moreover, extending this framework to include dynamic hand-object interactions, varying redirection strategies (e.g., rotation, scaling), and real-world applications like MR drawing or manipulation tasks could broaden the applicability of MR hand redirection in practical settings.

## ACKNOWLEDGMENTS

This material is based upon work supported in part by the National Science Foundation under Grants No. 2219842, 2309564, 2212200, 2417510, 2318657.

## REFERENCES

- [1] M. Azmandian, M. Hancock, H. Benko, E. Ofek, and A. Wilson. Haptic retargeting: Dynamic repurposing of passive haptics for enhanced virtual reality experiences. In *Proceedings of the 2016 CHI Conference on Human Factors in Computing Systems*, pp. 1968–1979. ACM, 2016. [1](#), [2](#), [3](#), [4](#)
- [2] Y. Ban, T. Kajinami, T. Narumi, T. Tanikawa, and M. Hirose. Modifying an identified angle of edged shapes using pseudo-haptic effects. In *Haptics: Perception, Devices, Mobility, and Communication: International Conference, EuroHaptics 2012, Tampere, Finland, June 13-15, 2012. Proceedings, Part I*, pp. 25–36. Springer, 2012. [2](#)
- [3] Y. Ban, T. Kajinami, T. Narumi, T. Tanikawa, and M. Hirose. Modifying an identified curved surface shape using pseudo-haptic effect. In *2012 IEEE Haptics Symposium (HAPTICS)*, p. 211–216. IEEE, Mar. 2012. doi: [10.1109/haptic.2012.6183793](https://doi.org/10.1109/haptic.2012.6183793) [2](#)
- [4] Y. Ban, T. Narumi, T. Tanikawa, and M. Hirose. Modifying perceived size of a handled object through hand image deformation. *Presence: Teleoperators and Virtual Environments*, 22(3):255–270, 2013. [2](#)
- [5] Y. Ban, T. Narumi, T. Tanikawa, and M. Hirose. Controlling perceived stiffness of pinched objects using visual feedback of hand deformation. In *2014 IEEE Haptics Symposium (HAPTICS)*, pp. 557–562. IEEE, 2014. [2](#)

- [6] A. Bangor, P. Kortum, and J. Miller. Determining what individual sus scores mean: Adding an adjective rating scale. *Journal of usability studies*, 4(3):114–123, 2009. 7
- [7] B. Benda, S. Esmaeili, and E. D. Ragan. Determining detection thresholds for fixed positional offsets for virtual hand remapping in virtual reality. In *2020 IEEE International Symposium on Mixed and Augmented Reality (ISMAR)*, pp. 269–278. IEEE, 2020. 2
- [8] G. Bradski. OpenCV: Open source computer vision library. *Dr. Dobb's Journal of Software Tools*, 2000. 4
- [9] J. Brooke. SUS: A quick and dirty usability scale. *Usability Evaluation in Industry*, 1996. 5
- [10] G. Calvert, C. Spence, and B. E. Stein. *The handbook of multisensory processes*. MIT press, 2004. 2
- [11] L.-P. Cheng, E. Ofek, C. Holz, H. Benko, and A. D. Wilson. Sparse haptic proxy: Touch feedback in virtual environments using a general passive prop. In *Proceedings of the 2017 CHI Conference on Human Factors in Computing Systems*, pp. 3718–3728, 2017. 2
- [12] W. G. Cochran. The comparison of percentages in matched samples. *Biometrika*, 37(3/4):256–266, 1950. 6
- [13] J. Cohen. *Statistical power analysis for the behavioral sciences*. routledge, 2013. 5
- [14] M. Dennison and M. D’Zmura. Effects of unexpected visual motion on postural sway and motion sickness. *Applied ergonomics*, 71:9–16, 2018. 8
- [15] M. Feick, A. Zenner, S. Seibert, A. Tang, and A. Krüger. The impact of avatar completeness on embodiment and the detectability of hand redirection in virtual reality. In *Proceedings of the 2024 CHI Conference on Human Factors in Computing Systems*, pp. 1–9, 2024. 2
- [16] A. R. Fender and C. Holz. Causality-preserving asynchronous reality. In *Proceedings of the 2022 CHI Conference on Human Factors in Computing Systems*, pp. 1–15, 2022. 4
- [17] A. R. Fender, T. Roberts, T. Luong, and C. Holz. Infinitepaint: Painting in virtual reality with passive haptics using wet brushes and a physical proxy canvas. In *Proceedings of the 2023 CHI Conference on Human Factors in Computing Systems*, pp. 13–13, 2023. 4
- [18] T. Feuchtnet and J. Müller. Ownershipshift: Facilitating overhead interaction in virtual reality with an ownership-preserving hand space shift. In *Proceedings of the 31st Annual ACM Symposium on User Interface Software and Technology*, pp. 31–43, 2018. 2
- [19] A. Field. *Discovering statistics using IBM SPSS statistics*. Sage publications limited, 2024. 5
- [20] R. A. Fisher and R. A. Fisher. *The design of experiments*. Springer, 1971. 4
- [21] M. Friedman. The use of ranks to avoid the assumption of normality implicit in the analysis of variance. *Journal of the American Statistical Association*, 32(200):675–701, 1937. doi: [10.1080/01621459.1937.10503522](https://doi.org/10.1080/01621459.1937.10503522) 6
- [22] E. J. Gonzalez, P. Abtahi, and S. Follmer. Reach+: extending the reachability of encountered-type haptics devices through dynamic redirection in vr. In *Proceedings of the 33rd Annual ACM Symposium on User Interface Software and Technology*, pp. 236–248, 2020. 2
- [23] C. Groth, T. Scholz, S. Castillo, J.-P. Tauscher, and M. Magnor. Instant hand redirection in virtual reality through electrical muscle stimulation-triggered eye blinks. In *Proceedings of the 29th ACM Symposium on Virtual Reality Software and Technology*, pp. 1–11, 2023. 2
- [24] R. Gruen, E. Ofek, A. Steed, R. Gal, M. Sinclair, and M. Gonzalez-Franco. Measuring system visual latency through cognitive latency on video see-through ar devices. In *2020 IEEE Conference on Virtual Reality and 3D User Interfaces (VR)*, pp. 791–799. IEEE, 2020. 5
- [25] D. T. Han, M. Suhail, and E. D. Ragan. Evaluating remapped physical reach for hand interactions with passive haptics in virtual reality. *IEEE transactions on visualization and computer graphics*, 24(4):1467–1476, 2018. 1, 2
- [26] J. Hartfill, J. Gabel, L. Kruse, S. Schmidt, K. Riebandt, S. Kühn, and F. Steinicke. Analysis of detection thresholds for hand redirection during mid-air interactions in virtual reality. In *Proceedings of the 27th ACM Symposium on Virtual Reality Software and Technology*, pp. 1–10, 2021. 2, 3
- [27] J. Hartfill, M. Schrader, and F. Steinicke. Investigating the impact of virtual hand realism on embodiment and redirection sensitivity in virtual reality. In *GI VR/AR Workshop*, pp. 10–18420. Gesellschaft für Informatik eV, 2024. 2
- [28] M. Höll, M. Oberweger, C. Arth, and V. Lepetit. Efficient physics-based implementation for realistic hand-object interaction in virtual reality. In *2018 IEEE conference on virtual reality and 3D user interfaces (VR)*, pp. 175–182. IEEE, 2018. 1
- [29] Y.-H. Huang, Y.-T. Sun, Z. Yang, X. Lyu, Y.-P. Cao, and X. Qi. Scgs: Sparse-controlled gaussian splatting for editable dynamic scenes. In *Proceedings of the IEEE/CVF conference on computer vision and pattern recognition*, pp. 4220–4230, 2024. 3
- [30] Y. Jiang, C. Yu, T. Xie, X. Li, Y. Feng, H. Wang, M. Li, H. Lau, F. Gao, Y. Yang, et al. Vr-gs: A physical dynamics-aware interactive gaussian splatting system in virtual reality. In *ACM SIGGRAPH 2024 Conference Papers*, pp. 1–1, 2024. 3
- [31] R. S. Kennedy, N. E. Lane, K. S. Berbaum, and M. G. Lilienthal. Simulator sickness questionnaire: An enhanced method for quantifying simulator sickness. *The international journal of aviation psychology*, 3(3):203–220, 1993. 5
- [32] B. Kerbl, G. Kopanas, T. Leimkühler, and G. Drettakis. 3d gaussian splatting for real-time radiance field rendering. *ACM Transactions on Graphics (TOG)*, 42(4):1–14, 2023. 3, 9
- [33] S. Liao, S. Chaudhri, M. K. Karwa, and V. Popescu. Seamlessvr: Bridging the immersive to non-immersive visualization divide. *IEEE Transactions on Visualization and Computer Graphics*, 2025. 1
- [34] B. J. Matthews, C. Reichherzer, B. H. Thomas, and R. T. Smith. Maskwarp: Visuo-haptic illusions in mixed reality using real-time video inpainting. In *2023 IEEE International Symposium on Mixed and Augmented Reality Adjunct (ISMAR-Adjunct)*, pp. 767–768. IEEE, 2023. 3
- [35] B. J. Matthews, B. H. Thomas, G. S. Von Itzstein, and R. T. Smith. Towards applied remapped physical-virtual interfaces: Synchronization methods for resolving control state conflicts. In *Proceedings of the 2023 CHI Conference on Human Factors in Computing Systems*, pp. 1–18, 2023. 1, 2
- [36] T. Matthews and K. Caine. Remapped physical–virtual interfaces for spatial alignment in vr. In *Proceedings of the 2023 CHI Conference on Human Factors in Computing Systems*. ACM, 2023. 2
- [37] J. W. Mauchly. Significance test for sphericity of a normal n-variate distribution. *The Annals of Mathematical Statistics*, 11(2):204–209, 1940. doi: [10.1214/aoms/1177731915](https://doi.org/10.1214/aoms/1177731915) 6
- [38] Q. McNemar. Note on the sampling error of the difference between correlated proportions or percentages. *Psychometrika*, 12(2):153–157, 1947. 6
- [39] B. Mildenhall, P. P. Srinivasan, M. Tancik, J. T. Barron, R. Ramamoorthi, and R. Ng. Nerf: Representing scenes as neural radiance fields for view synthesis. In *ECCV*, pp. 405–421. Springer, 2020. 3, 9
- [40] R. A. Montano Murillo, S. Subramanian, and D. Martinez Plasencia. Erg-o: Ergonomic optimization of immersive virtual environments. In *Proceedings of the 30th annual ACM symposium on user interface software and technology*, pp. 759–771, 2017. 2
- [41] M. Moran-Ledesma, O. Schneider, and M. Hancock. User-defined gestures with physical props in virtual reality. *Proceedings of the ACM on Human-Computer Interaction*, 5(ISS):1–23, 2021. 1
- [42] S. Mori, S. Ikeda, and H. Saito. A survey of diminished reality: Techniques for visually concealing, eliminating, and seeing through real objects. *IPSJ Transactions on Computer Vision and Applications*, 9:1–14, 2017. 3
- [43] K. Ogawa, K. Fujita, K. Takashima, and Y. Kitamura. Redirected drawing: Expanding the perceived canvas size in vr. In *2025 IEEE Conference on Virtual Reality and 3D User Interfaces (VR)*, pp. 494–504. IEEE, 2025. 2
- [44] M. Ogawa, K. Matsumoto, K. Aoyama, and T. Narumi. Expansion of detection thresholds for hand redirection using noisy tendon electrical stimulation. In *2023 IEEE International Symposium on Mixed and Augmented Reality (ISMAR)*, pp. 1026–1035. IEEE, 2023. 2
- [45] N. Ogawa, T. Narumi, and M. Hirose. Effect of avatar appearance on detection thresholds for remapped hand movements. *IEEE transactions on visualization and computer graphics*, 27(7):3182–3197, 2020. 2, 8
- [46] J. L. Ponton, R. Keshavarz, A. Beacco, and N. Pelechano. Stretch your reach: Studying self-avatar and controller misalignment in virtual reality interaction. In *Proceedings of the 2024 CHI Conference on Human Factors in Computing Systems*, pp. 1–15, 2024. 2
- [47] N. Prins et al. *Psychophysics: a practical introduction*. Academic Press, 2016. 5, 6
- [48] E. D. Ragan, S. Scerbo, F. Bacim, and D. A. Bowman. Amplified head rotation in virtual reality and the effects on 3d search, training transfer, and spatial orientation. *IEEE transactions on visualization and computer graphics*, 23(8):1880–1895, 2016. 8
- [49] S. S. Shapiro and M. B. Wilk. An analysis of variance test for normality (complete samples). *Biometrika*, 52(3/4):591–611, 1965. 6

- [50] C. Spearman. The proof and measurement of association between two things. *The American Journal of Psychology*, 15(1):72–101, 1904. doi: [10.2307/1412159](https://doi.org/10.2307/1412159) 6
- [51] J.-P. Stauffert, F. Niebling, and M. E. Latoschik. Effects of latency jitter on simulator sickness in a search task. In *2018 IEEE conference on virtual reality and 3D user interfaces (VR)*, pp. 121–127. IEEE, 2018. 3
- [52] K. Tanaka, T. Nakamura, K. Matsumoto, H. Kuzuoka, and T. Narumi. Detection thresholds for replay and real-time discrepancies in vr hand redirection. *IEEE Transactions on Visualization and Computer Graphics*, 2025. 2
- [53] Y. Tanaka, A. Shen, A. Kong, and P. Lopes. Full-hand electro-tactile feedback without obstructing palmar side of hand. In *Proceedings of the 2023 CHI Conference on Human Factors in Computing Systems*, pp. 1–15, 2023. 1
- [54] R. Venkatakrishnan, R. Venkatakrishnan, R. Canales, B. Raveendranath, C. C. Pagano, A. C. Robb, W.-C. Lin, and S. V. Babu. Investigating the effects of avatarization and interaction techniques on near-field mixed reality interactions with physical components. *IEEE Transactions on Visualization and Computer Graphics*, 2024. 2
- [55] R. Venkatakrishnan, R. Venkatakrishnan, B. Raveendranath, C. C. Pagano, A. C. Robb, W.-C. Lin, and S. V. Babu. Give me a hand: Improving the effectiveness of near-field augmented reality interactions by avatarizing users' end effectors. *IEEE Transactions on Visualization and Computer Graphics*, 29(5):2412–2422, 2023. 2, 9
- [56] E. Whitmire, H. Benko, C. Holz, E. Ofek, and M. Sinclair. Haptic revolver: Touch, shear, texture, and shape rendering on a reconfigurable virtual reality controller. In *Proceedings of the 2018 CHI conference on human factors in computing systems*, pp. 1–12, 2018. 1
- [57] F. Wilcoxon. Individual comparisons by ranking methods. *Biometrics Bulletin*, 1(6):80–83, 1945. doi: [10.2307/3001968](https://doi.org/10.2307/3001968) 6
- [58] G. Wu, T. Yi, J. Fang, L. Xie, X. Zhang, W. Wei, W. Liu, Q. Tian, and X. Wang. 4d gaussian splatting for real-time dynamic scene rendering. In *Proceedings of the IEEE/CVF conference on computer vision and pattern recognition*, pp. 20310–20320, 2024. 3
- [59] P. Xiong, Y. Zhang, N. Zhang, S. Fu, X. Li, Y. Zheng, J. Zhou, X. Hu, and M. Fan. To reach the unreachable: Exploring the potential of vr hand redirection for upper limb rehabilitation. In *Proceedings of the 2024 CHI Conference on Human Factors in Computing Systems*, pp. 1–11, 2024. 2
- [60] R. Yao, T. Heath, A. Davies, T. Forsyth, N. Mitchell, and P. Hoberman. *Oculus VR Best Practices Guide*. Oculus VR, Inc., 2014. Accessed: 2025-06-10. 5
- [61] A. Zenner, C. Karr, M. Feick, O. Ariza, and A. Krüger. Beyond the blink: Investigating combined saccadic & blink-suppressed hand redirection in virtual reality. In *Proceedings of the 2024 CHI Conference on Human Factors in Computing Systems*, pp. 1–14, 2024. 2
- [62] A. Zenner, H. M. Kriegler, and A. Krüger. Hart-the virtual reality hand redirection toolkit. In *Extended Abstracts of the 2021 CHI Conference on Human Factors in Computing Systems*, pp. 1–7, 2021. 2, 4
- [63] A. Zenner and A. Krüger. Drag: on: A virtual reality controller providing haptic feedback based on drag and weight shift. In *Proceedings of the 2019 CHI Conference on Human Factors in Computing Systems*, pp. 1–12, 2019. 1
- [64] A. Zenner and A. Krüger. Estimating detection thresholds for desktop-scale hand redirection in virtual reality. In *2019 IEEE Conference on Virtual Reality and 3D User Interfaces (VR)*, pp. 47–55. IEEE, 2019. 1, 3
- [65] A. Zenner, K. P. Regitz, and A. Krüger. Blink-suppressed hand redirection. In *2021 IEEE Virtual Reality and 3D User Interfaces (VR)*, pp. 75–84. IEEE, 2021. 2
- [66] Y. Zhou and V. Popescu. Tapping with a handheld stick in vr: Redirection detection thresholds for passive haptic feedback. In *2022 IEEE Conference on Virtual Reality and 3D User Interfaces (VR)*, pp. 83–92. IEEE, 2022. 1
- [67] Y. Zhou and V. Popescu. Dynamic redirection for vr haptics with a handheld stick. *IEEE Transactions on Visualization and Computer Graphics*, 29(5):2753–2762, 2023. 3
- [68] Y. Zhou and V. Popescu. Detectability of ethd position and speed redirection for vr haptics. In *2024 IEEE International Symposium on Mixed and Augmented Reality (ISMAR)*, pp. 140–149. IEEE, 2024. 1
- [69] Y. Zhou and V. Popescu. Dynamic redirection for safe interaction with ethd-simulated virtual objects. *IEEE Transactions on Visualization and Computer Graphics*, 2025. 1